New Detections of Feldspar-Bearing Volcanic Rocks in the Walls of Valles Marineris, Mars

Jessica Flahaut, Vincent Payet, Frank Fueten, Martin Guitreau, Marie Barthez, Gen Ito, Pascal Allemand

Geophysical Research Letters

RESEARCH LETTER
10.1029/2022GL100772

Key Points:

- Eight new detections of plagioclase-like signatures are reported in their original geologic context in the walls of Valles Marineris
- At one location, the possible feldspar signatures are clearly associated with a 200 m thick sub-horizontal layer, hinting at an eruptive origin
- Plagioclase detections on Mars are uncommon but include multiple lithologies, with various implications for magmatic processes

Supporting Information:

Supporting Information may be found in the online version of this article.

Correspondence to:

J. Flahaut,
jessica.flahaut@unvi-lorraine.fr

Citation:

Flahaut, J., Payet, V., Fueten, F., Guitreau, M., Barthez, M., Ito, G., & Allemand, P. (2023). New detections of feldspar-bearing volcanic rocks in the walls of Valles Marineris, Mars. *Geophysical Research Letters*, *50*, e2022GL100772. https://doi.org/10.1029/2022GL100772

Received 11 AUG 2022
Accepted 16 DEC 2022

New Detections of Feldspar-Bearing Volcanic Rocks in the Walls of Valles Marineris, Mars

Jessica Flahaut[1], Vincent Payet[1,2], Frank Fueten[3], Martin Guitreau[4], Marie Barthez[1], Gen Ito[1], and Pascal Allemand[5]

[1]Centre de Recherches Pétrographiques et Géochimiques (CRPG), CNRS UMR7358/Université de Lorraine, Vandœuvre-lès-Nancy, France, [2]Institut Pierre Simon Laplace, CNRS, Palaiseau, France, [3]Department of Earth Sciences, Brock University, St. Catharines, ON, Canada, [4]Université Clermont Auvergne, Laboratoire Magmas et Volcans, OPGC, CNRS UMR 6524, IRD UMR163, Clermont-Ferrand, France, [5]Laboratoire de Géologie de Lyon: Terre, Planète, Environnement (LGL, TPE), Université Lyon 1/CNRS, Villeurbanne Cedex, France

Abstract Plagioclase-bearing rocks were first detected in the vicinity of large impact basins on Mars using visible/near-infrared (VNIR) data. The geologic context is consistent with excavated plutons or ancient crustal outcrops. Our analyses reveal plagioclase outcrops exposed in a 200 m thick, sub-horizontal layer in the 8 km deep walls of the Valles Marineris canyon. These plagioclase-bearing rocks are consistent with either a sill, a volcano-clastic layer, or a porphyritic lava flow, in contrast with the previous understanding that plagioclase feldspar signatures must be indicative of nearly pure, anorthositic rocks inherited from a primary flotation crust or granitoids from either plutonic activity or ancient continental crust. We present here evidence of possibly effusive, volcanic rocks bearing plagioclase VNIR spectral signatures, expanding the geologic setting of these unique and uncommon martian rocks to include multiple lithologies. This has direct implications for Mars magmatic processes and for the nature of its crust.

Plain Language Summary Detection of plagioclase feldspar minerals from remote sensing instruments onboard Mars missions is difficult, and only a handful of occurrences have been reported so far. We present here new detections of such minerals in the giant Martian canyon of Valles Marineris (VM), exposed in their original context, and associated at least in one location, to a 200 m thick sub-horizontal layer within the walls. Analyses were performed using visible near-infrared spectral data, which are commonly compared to reference spectra of known terrestrial minerals, or mineral powders, acquired in the laboratory. Whereas previous detections were interpreted as evidence for plagioclase-dominated, or at least, nearly mafic-free, plutonic rocks, we argue here that the VM outcrops correspond to erupted, volcanic products. The signature of plagioclase could originate from large crystals hosted in mafic, intermediate, or felsic volcanic rocks; from a lava flow, or from welded ashes. Our new observations confirm that plagioclase detections on Mars can correspond to multiple types of rocks and bring more clues to ongoing debates regarding the extent of Mars magmatic processes and the nature of its crust.

1. Introduction

Visible-Near infrared (VNIR) spectroscopy has led to many discoveries pertaining to Mars geologic history (e.g., the discovery of hydrated minerals associated with ancient terrains with the Observatoire pour la Minéralogie, l'Eau, les Glaces et l'Activité, OMEGA, Bibring et al., 2006). Felsic materials are difficult to identify with VNIR spectroscopic techniques, as quartz and feldspar are nominally undetectable in the VNIR domain (~0.4–3.9 μm) where both OMEGA and CRISM (the Compact Reconnaissance Imaging Spectrometer for Mars) operate. Felsic materials are more easily identified in the thermal infrared range (e.g., Rogers & Nekvasil, 2015) although the lower spatial resolutions of instruments like the Thermal Emission Spectrometer and the Thermal Emission Imaging System (THEMIS) preclude analyses of small-scale outcrops. Yet, some feldspars, especially plagioclase, may exhibit a weak, broad absorption band centered at 1.25–1.31 μm due to minor substitutions of Ca^{2+} by Fe^{2+} (e.g., Adams & Goullaud, 1978). Previous lunar analog laboratory studies showed, however, that when mixing powders of Ca plagioclase with a mafic component, the feldspar absorption band becomes hidden at low olivine and pyroxene content (Cheek & Pieters, 2014; Crown & Pieters, 1987; Nash & Conel, 1974). Cheek and Pieters (2014) further demonstrated that the 1.3 μm feature is only detectable if the plagioclase modal abundance is >90%. Therefore, previous VNIR feldspar detections on Mars have been tentatively interpreted as evidence for

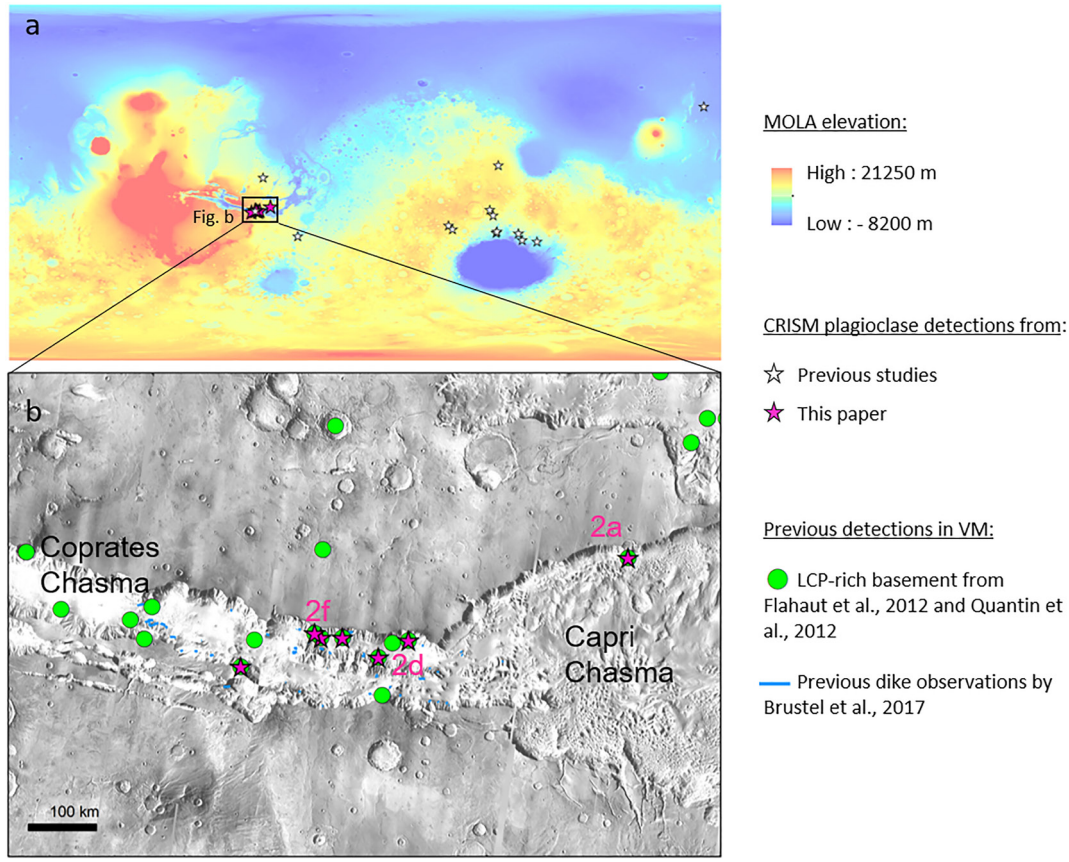

Figure 1. (a) CRISM plagioclase detections on Mars (White stars: compilation from Carter & Poulet (2013), Wray et al. (2013), Viviano-Beck et al. (2017), Farrand et al. (2021), Rogers & Farrand (2022), Phillips et al. (2022), Magenta stars: this paper). The background colors represent the Mars Orbiter Laser Altimeter global elevation map of Mars in rainbow scale. (b) Close-up of the Valles Marineris (VM) area. Previous detections of a low-calcium pyroxene (LCP)-rich bedrock identified both in the lower walls of VM (Flahaut et al., 2012) and in the surrounding impact craters (Quantin et al., 2012) are indicated by green circles. Dike observations in the walls of Coprates Chasma (Brustel et al., 2017) are also reported as blue lines. The background is the THEMIS IR Day mosaic of Mars in grayscale (see text for references).

nearly ferro-magnesian-mineral-free rocks such as pure anorthositic (Carter & Poulet, 2013; Phillips et al., 2022) or granitic (Wray et al., 2013) rocks. Most of the aforementioned detections are located in the vicinity of large impact basins, such as Hellas and Argyre, which suggests that these rocks could have been excavated from greater depths. Consequently, the stratigraphic position and geologic context of these feldspar-bearing rocks is poorly constrained.

Most recent detections of feldspar-bearing rocks with CRISM, associated with low (<60 wt%) to intermediate silica contents according to THEMIS, widen the range of context and possible lithologies (Farrand et al., 2021; Rogers & Farrand, 2022). Plagioclase felspar signatures associated with a dome-like feature in western Arcadia Planitia (Farrand et al., 2021), and to lava flows in Nili Patera (Rogers & Farrand, 2022), suggest that plagioclase signatures can be detected in association with effusive or intrusive eruptive products. These observations confirm the assumption of Rogers and Nekvasil (2015) that porphyritic igneous rocks with less than 90% feldspars can present diagnostic plagioclase absorption in their VNIR spectra.

We present here new feldspar signatures detected on eight CRISM observations acquired on the walls of the VM canyon system on Mars (Figures 1a and 1b), review their geologic context, and discuss their possible lithologies and implications for Mars magmatic processes.

2. Materials and Methods

2.1. Data Set

A range of remote sensing data set from Mars missions was collected, processed and assembled in a Geographic Information System for further analyses. The Mars Orbiter Laser Altimeter (MOLA) elevation and THEMIS IR day global maps were downloaded from the US Geological Survey (USGS) Astropedia website (Edwards et al., 2011; Smith et al., 2001). Data from the High Resolution Imaging Science Experiment (HiRISE), Context Camera (CTX), and CRISM instruments were downloaded as calibrated and map-projected products from the MarsSI web application (Quantin-Nataf et al., 2018).

CTX and HiRISE Digital Terrain Model (DTM) were computed from stereo-pairs D22_035911_1651_XN_14S057W/F02_036689_1660_XN_14S057W and PSP_010277_1650_RED/PSP_010699_1650_RED respectively, using the NASA AMES stereo-pipeline on ISIS3 (Beyer et al., 2018). Layer dips and thickness were measured on the CTX and HiRISE DTM using the Orion software (Pangaea Scientific, 2006), after fitting a plane trace to the upper and lower boundary of the outcrop (Fueten et al., 2008).

2.2. Mineral Identification With CRISM

Standard processing approaches were used to correct CRISM data from photometric and atmospheric effects using the volcano scan technique (e.g., McGuire et al., 2009) and CRISM Analysis Toolkit for ENVI (@Harris Geospatial, Murchie et al., 2007). In addition, CRISM data were cleaned from residual noise using a custom-made routine known as Mineral Recognizer (Payet et al., 2020). The python-based Mineral Recognizer software can be used to denoise hyperspectral signals and compute spectral criteria on large multi or hyper spectral data. Mineral Recognizer allows implementation of various customized denoising methods; all the spectra presented here were cleaned using ordinary kriging with a linear variogram model, although other proposed algorithms (e.g., natural spline, moving median) yield similar results. Figure S1 in Supporting Information S1 shows the difference between raw spectra and cleaned spectra processed with Mineral Recognizer. A clear advantage of the software is to provide a cleaned data set on which it is easier to identify weak signatures, although raw data were always verified for consistency.

Plagioclase feldspar minerals are detected in the CRISM spectral cubes by deriving the spectral index referred to as BD1300 based on band math comparing the reflectance value of the band center around 1.3 μm and its shoulders (BD1300 = 1–R1320/(0.642*R1080 + 0.358*R1750), with Rxxxx indicating the reflectance value at wavelength xxxx in nm). The same approach is used to identify associated hydrous and mafic minerals, using the set of CRISM spectral parameters developed by Viviano-Beck et al. (2014). CRISM spectral parameters were then computed on both raw and cleaned data; the cleaned data resulted in smoother images with less background noise. Although band depths are related to mineral abundances, the spectral parameters may also be sensitive to environmental effects such as changing illumination, topography, the geometry of data acquisition and instrumental noise. For this reason, all spectra in pixels with positive BD1300 were manually checked to confirm the presence of a 1.3 μm feldspar absorption band.

An additional step often carried out when analyzing Mars CRISM spectra is spectral ratioing: spectral ratioing is used to remove residual artifacts from imperfect radiometric and atmospheric corrections and enhance spectral features of interest by dividing the spectra of a region of interest from the one of spectrally neutral area (e.g., Viviano-Beck et al., 2014). As noted by Carter and Poulet (2013), spectral ratioing using a denominator with pyroxene signatures may induce a false feldspar-like absorption band. Therefore, we reject spectra that do not show flat spectral slope between 1.7 and 2.65 μm, have slight positive slope, or have positive pyroxene spectral parameters (LCPIndex2 or HCPindex2) as possible denominators.

Both raw and ratioed spectra were compared with reference spectra from previous Mars CRISM detections from Carter and Poulet (2013), with spectra of known terrestrial anorthite samples from the USGS reference library (Kokaly et al., 2017), and with lunar anorthosite spectra from the returned Apollo samples available in the RELAB spectral library (Milliken et al., 2016).

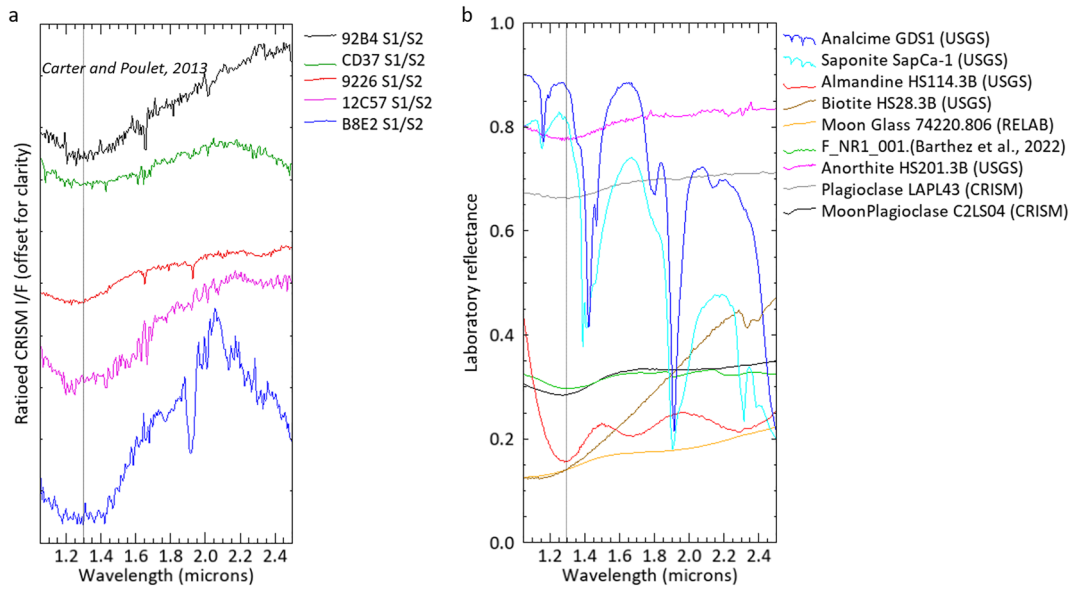

Figure 2. (a) CRISM spectra of feldspar -like absorptions, plotted against from the previous Mars CRISM detections of Carter and Poulet (2013). Displayed spectra are ratioed spectra from raw CRISM data cubes (see pixel coordinates, numerators and denominators in Figure S2 in Supporting Information S1). A vertical line at 1.3 μm indicates the expected band center for the broad, weak plagioclase feldspar absorption. (b) Reference spectra from the USGS, CRISM, and RELAB libraries, as well as the spectrum of a terrestrial porphyritic basalt (Barthez et al., 2022) are shown for comparison.

3. Results

3.1. Spectroscopic Detections of Plagioclase Feldspar

Plagioclase feldspars are detected over 8 CRISM observations in the mid to lower walls of the well-exposed, 8 km high Coprates and Capri Chasmata (Figure 2). All these detections are associated with the Fe/Mg phyllosilicate-rich wall layer and low calcium pyroxene (LCP)-rich light-toned bedrock previously described by Flahaut et al. (2012) (Figure 1b). The position of the observed Fe^{2+} band is centered around ∼1.30 μm in all spectra, suggesting little compositional/grain size/ferro-magnesian mineral or phyllosilicate content variability. Although the left shoulder of the plagioclase is not visible on the CRISM NIR data (1–3.92 μm), the position of the right shoulder at ∼1.6 μm is consistent with both previous detections (e.g., Carter & Poulet, 2013) and from reference spectra from terrestrial anorthite. Although other minerals from the spectral library (e.g., garnet, amphibole, biotite, Fe-rich olivine) and volcanic glass may exhibit broad absorptions centered around 1.2–1.3 μm, the different shape, shoulder positions of the band and the absence of other diagnostic bands expected for these minerals support our interpretation of the VM signatures tracking plagioclase feldspar (Figure 2). Additional bands at 1.91 and 2.31 μm diagnostic of Fe/Mg smectites are visible in most of the feldspar-bearing spectra, while spectra from observations FRT000B8E2 also exhibits absorptions at 2.12, 2.50 and a water band at 1.90 μm indicative of zeolites, possibly mixed with carbonates at this location (Viviano-Beck et al., 2017) (Figure 2).

3.2. Geological Context

All feldspar detections were made at MOLA elevations between −3,500 m and −1,100 m in the middle to lower walls of the canyon. Since most detections are limited to a few CRISM pixels, it is often difficult to identify the layer or outcrop carrying the signature from high-resolution CTX and HiRISE images. At six locations, feldspar signatures occur within the clay-bearing layer, suggesting that the dual signatures in spectra could result from a spatial mixture within the CRISM pixel of 18 m and not necessarily from feldspar alteration to clays (which would more likely result in the formation of Al-clays; Figures 3a–3c,3f, and 3g). We cannot exclude, however, that the feldspar-bearing rock, especially if mafic, is altered into Fe/Mg smectites and that both feldspars and smectites are hosted in the same parent rock. Feldspars detected at two locations are associated with light-toned bedrocks of the lower walls of VM (Figures 3d and 3e): the plagioclase-dominated spectra are then observed within the bedrock layer whose pixels are more commonly dominated by LCP signatures (Flahaut et al., 2012).

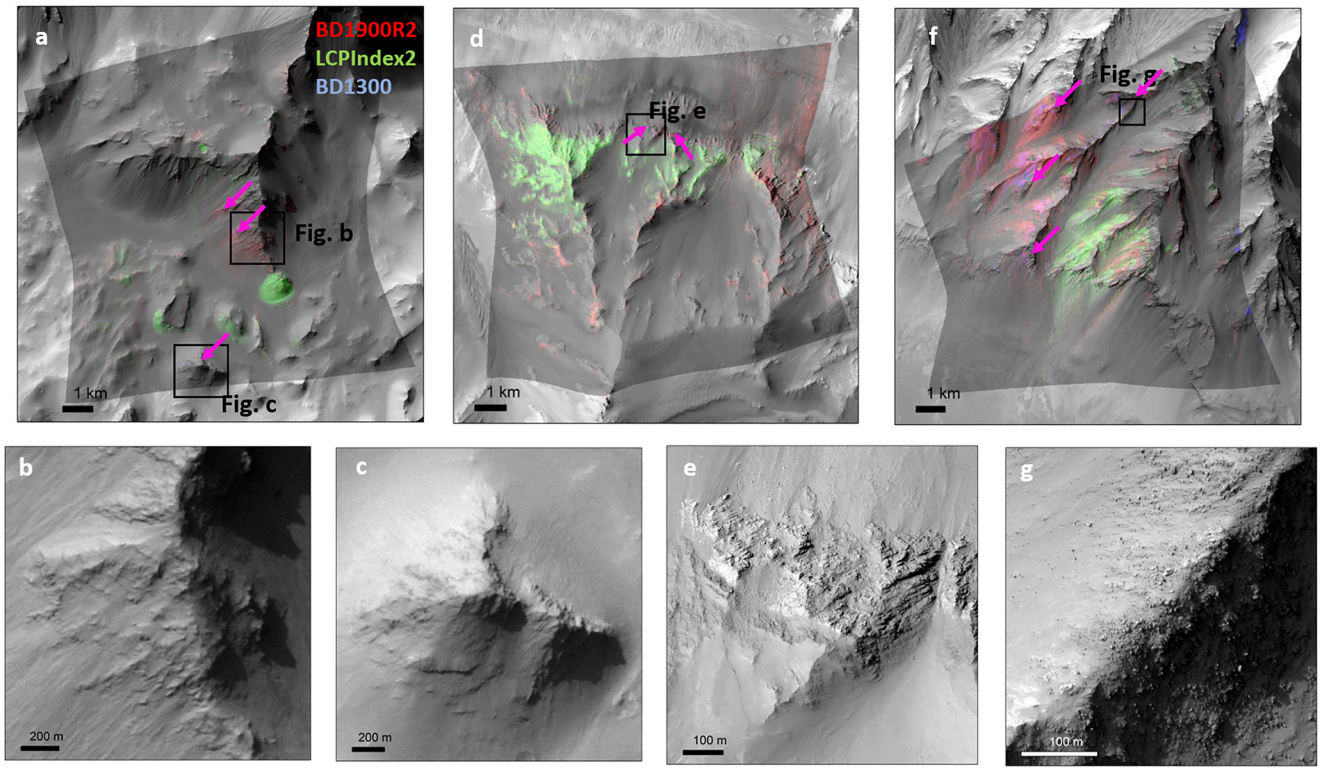

Figure 3. a- CRISM FRT00008112 color composite of image summary parameters R = BD1900R2, G = LCPINDEX2 and B= BD1300 are projected in transparency over CTX image F20_043546_1695_XN_10S048W of the northern walls of Capri Chasma. This color composite highlights LCP-rich bedrock outcrops in green, clay-bearing outcrops in red and mixed clays and feldspars in magenta (see arrows as well). (b, c) Close-ups on feldspar-bearing outcrops on the same CTX image. (d) CRISM FRT00009226 RGB composite of the same summary parameters are projected in transparency over CTX image P15_006717_1643_XI_15S054W. e-Close-up on feldspar-bearing outcrops on corresponding High Resolution Imaging Science Experiment (HiRISE) image PSP_006717_1655 (f) CRISM FRT0000B8E2 RGB composite of the same summary parameters are projected in transparency over CTX image P15_006717_1643_XI_15S054W. (g) Close-up of feldspar-bearing outcrops on corresponding HiRISE image PSP_009222_1660.

Previous studies reported the presence of this higher albedo bedrock buried below 3–4 km of lava flows in the walls of VM, and tentatively interpreted it as a large igneous intrusion (Williams et al., 2003) or remnants of an ancient Noachian crust (Flahaut et al., 2012).

On CRISM observation HRL0000CD37 in the southern wall of Coprates Chasma, the feldspar detection is more extended than in other observations and associated with a horizontal layer within the wall (Figure 4). Two planes following the upper and lower limit of the layer can be traced on both the CTX and HiRISE DTM over a distance of ~4 km with a maximum deviation of 15 m for a 2 km plane long trace. Strike and dip measurements on the HiRISE DTM indicate that the feldspar bearing layer is ~200 m thick and gently dipping (11° ± 4 for its upper boundary, 12° ± 3 for its lower boundary) to the north, toward the center of the canyon (Figures 4d and 4e). This dip trend is commonly observed for layers in the walls of VM (Fueten et al., 2005). Hundreds of dikes with distinct borders have been reported at the same location of VM (Brustel et al., 2017; Flahaut et al., 2011), however, no evidence for contact metamorphism is observed here. The clear morphology of this outcrop suggests that the feldspar signatures are carried either by a sedimentary/volcanoclastic layer, lava flow or a sill. This layer is blockier and more competent in appearance compared to the rest of the wall material, and can be traced continuously for several kilometers. The layer does not show a distinct albedo compared to the surrounding lavas of the wall.

4. Discussion and Conclusions

The geological context of most feldspar detections suggests that the plagioclase-bearing rock could be an explosive or effusive eruptive product, such as an ignimbrite sheet, or a lava flow. This hypothesis is supported by Figure 2 which shows the VNIR spectra of a basalt from Afar (F_NR1_001), Ethiopia (Pik et al., 1998), which

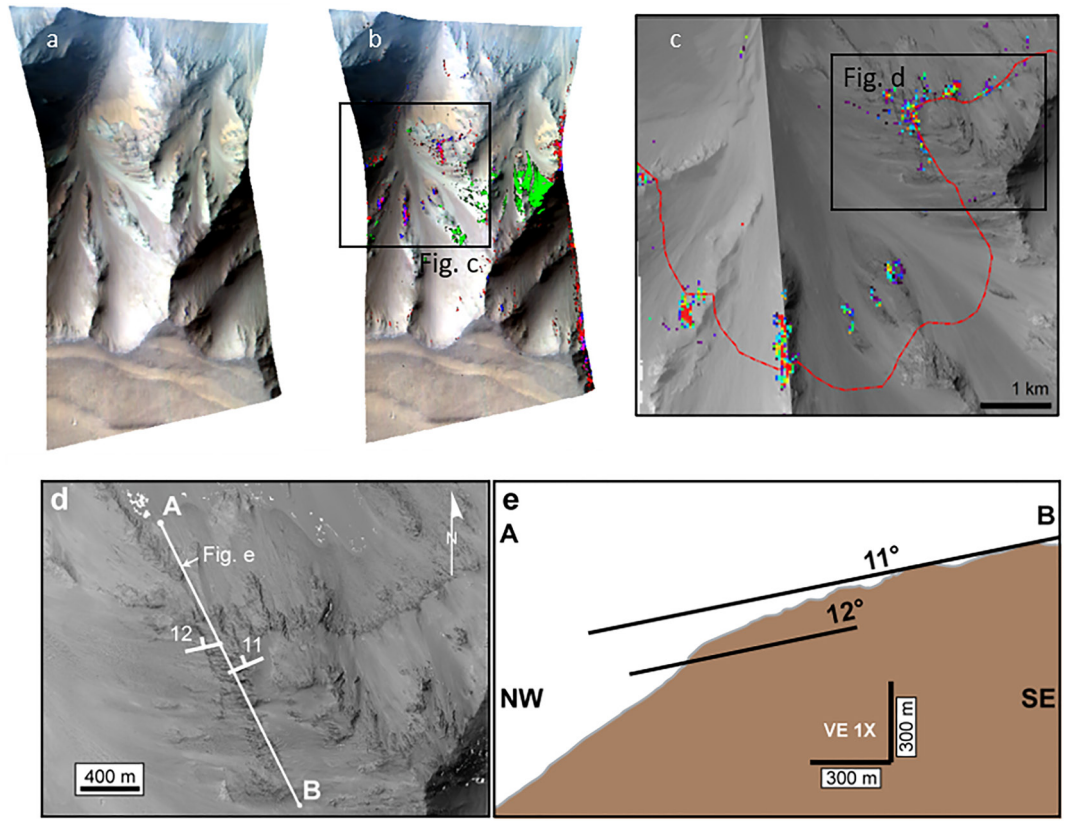

Figure 4. (a) Map-projected CRISM HRL0000CD37 false color composite (default bands, $R = 2.5295$ μm, $G = 1.5066$ μm, $B = 1.0800$ μm) with North to the top. The southern part of the image shows the top of the southern plateaus. (b) The RGB composite of summary parameters R = D2300, G = LCPIndex2, B=BD1300 is projected on top of the previous image (values <0 were masked). Green pixels indicate the location of low-calcium pyroxene signatures, whereas purple pixels indicate the location of mixed clays and plagioclase feldspar signatures. (c) The BD1300 spectral index is displayed in rainbow scale (blue = low, red = high) on top of corresponding High Resolution Imaging Science Experiment and CTX imagery. The red line indicates the trace of the top layer of the 200 m thick outcrop bearing the signature, as fitted on the CTX Digital Terrain Model, using the yellow points and a planar shape. Positive values of the BD1300 criteria follow this plane. (d) Dip and azimuth of the bounding top and lower layers were measured using the Orion software. (e) Cross-section along the white A-B line of (d): feldspar signatures are associated with a ~200 m thick layer bounded by two parallel planes gently dipping at 11–12° toward the north.

contains 1–8 mm plagioclase phenocrysts and plagioclase microlites, acquired with an ASD fieldspec 4 VNIR spectrometer (Barthez et al., 2022). The spectra display the broad ~1.3 μm band typical of plagioclase despite feldspar phenocrysts accounting for less than 50% of the rock (other minerals include altered olivine, and a matrix containing both feldspar and olivine-pyroxene microlitic crystals and rare oxides). Similar results were obtained when mixing large plagioclase crystals (>~840 μm) with as much as 50 vol % of ferro-magnesian minerals (Rogers & Nekvasil, 2015). More recently, analog studies of the Atacama Desert of northern Chile reported plagioclase-like signatures in the VNIR remote sensing data set of dacitic domes and ignimbrite sheets (Ito et al., 2022). We therefore conclude that materials with relatively large plagioclase crystals, such as porphyritic basalts (or more evolved effusive rocks) and/or with few mafic minerals, such as ignimbrite sheets, could be consistent with some of the weaker feldspathic detections identified from VNIR data, such as those in VM. As previously stated by Rogers and Nekvasil (2015), our conclusions contradict the assumption that very low (<5–10%) olivine and pyroxene contents are required in order to observe feldspar (plagioclase) signatures which was based on previous studies that determined the detection limit of plagioclase in VNIR spectra using mixtures of minerals with grain sizes <500 μm, for comparison to the Moon (e.g., Cheek & Pieters, 2014).

Determining the nature of the rocks bearing these rare, sporadic detections of feldspars is key to understanding Mars magmatic history. Previous interpretations as granitic or anorthositic rocks, which did not consider the impact of grain sizes on spectral signatures, have sharply different implications for Mars history. On one

hand, Carter and Poulet (2013) interpreted the plagioclase signatures as evidence for anorthositic rocks, which could represent remnants of a lunar-like flotation crust. The hypothesis of a primary feldspathic crust inherited from a magma ocean crystallization contrasts with existing models which suggest Mars primary crust was inherited from mantle overturn and subsequent Mg-rich cumulate melting, and thus, the primary crust of Mars should be basaltic (Elkins-Tanton et al., 2005) or andesitic (Bouvier et al., 2018) in composition. On the other hand, Wray et al. (2013) suggested that feldspar detection could be associated with granitoid plutons. Granodiorite with evolved feldspar compositions was also detected in situ by the Curiosity rover in Gale crater (Sautter et al., 2015, 2016) and tentatively interpreted as evidence for continental crust on Mars. Since Mars shows no evidence for plate tectonics, the existence of a possible tertiary crust is puzzling, although a number of other processes could be responsible for the formation of granitoids on Mars. These processes involve partial melting of an early basaltic crust in the presence of volatiles, extreme fractional crystallization of mafic magmas, specific tectonic setting (such as for the formation of Icelandites), or hydrous melting of the Martian mantle (Sautter et al., 2016).

A previous detection made by Viviano-Beck et al. (2017) tentatively interpreted the plagioclase signature as part of the Noachian crust. In the present study, we find feldspar signatures at different elevation of the walls: at 6 locations, plagioclase signatures occur within the boulder-rich,clay-rich layer of the middle walls, whereas at 2 locations, feldspars are detected within the deeper LCP-bearing crustal bedrock. We cannot exclude that feldspar signatures in VM could be associated with different lithologies, as this is likely the case for previous detections made on MarsDetections associated with the crustal bedrock could represent more plagioclase-rich banded layers within the LCP-dominated bedrock, which could be noritic or gabbroic in nature, as previously suggested in Flahaut et al. (2012), or magmatic intrusions. By contrast, most feldspar detections in VM appear more consistent with volcanic products and, hence, secondary crust rocks, which have different implications for Mars magmatic processes. Most basalts at the surface of Mars are relatively Al-poor compared to terrestrial ones (McSween et al., 2003, 2009). The presence of porphyritic effusive rocks in VM may evidence for a more Al-rich source but could also imply varying conditions in the magma chamber at the time of emplacement of this specific flow or sill. Assuming that the feldspar-bearing layer is a flow exposed in its original stratigraphic sequence, it would be older than the spectrally blank, top-layer of basaltic flows in the walls of VM (Flahaut et al., 2012). Varying pressure conditions, residence time, mixing, and emission rates are among the different factors that could explain the presence of plagioclase phenocrysts in the specific layer of Figure 4, and not in the rest of the wall's sequence. If the layer instead corresponds to an intrusive sill, it would be difficult to date, however, most dikes reported in VM are estimated to be Noachian in age (Brustel et al., 2017; Flahaut et al., 2011). We also cannot exclude that the layer has a more evolved composition than basalt (such as trachyte or dacite), or a volcanoclastic origin; these are more explosive eruptive styles, but the prevalence of feldspar signatures suggests the presence of phenocrysts, or the paucity of non-mafic minerals. Associated detections of Fe/Mg smectites and plagioclases signatures in VM could support the interpretation of a relative mafic, possibly effusive, rock. Visible/near-infrared plagioclase signatures in VM could therefore correspond to a number of possible lithologies, but seem to be associated with volcanic eruptive products at most locations. Associated mineral detections, as well as terrestrial analog studies and laboratory work, should help identify the range of possible contexts in the near future. A future mission to feldspar-bearing terrain locations, such as VM, would be also extremely helpful to constrain the lithology of these rocks (e.g., Fraeman et al., 2022).

Data Availability Statement

MOLA and THEMIS IR day global maps were downloaded from the USGS Astropedia website (https://astrogeology.usgs.gov/search). CRISM, HiRISE and CTX data are all available publicly on the Planetary Data System (PDS) archive, at https://pds-geosciences.wustl.edu/dataserv/mars.html. Generated CTX and HiRISE DTMs and associated images can be downloaded from the Brock University data repository, at the following address: http://hdl.handle.net/10464/16885. Reference spectra from this study can be downloaded from the open-access Mirabelle database on the Solid Spectroscopy Hosting Architecture of Databases and Expertise (SSHADE) platform (https://www.sshade.eu/db/mirabelle) (F_NR1_001 spectrum), the USGS (https://crustal.usgs.gov/speclab/QueryAll07a.php) or the RELAB (https://pds-geosciences.wustl.edu/spectrallibrary/default.htm) spectral libraries.

Acknowledgments
We are grateful to the Mars Reconnaissance Orbiter team for the availability of the data. This study was supported by the CNRS Momentum, LUE future leader programs, and the French "Program National de Planétologie" through grants attributed to J. Flahaut. The authors acknowledge the support of the French Agence Nationale de la Recherche (ANR), under Grant ANR-21-CE49-0003 (MARS-Spec). The component of the work by Frank Fueten was funded by an NSERC discovery grant. CRISM data have been processed with the MarsSI (marssi.univ-lyon1.fr) application founded by the European Union's Seventh Framework Program (FP7/2007–2013) (ERC Grant Agreement No. 280168). The authors would like to thanks the editor, the anonymous reviewer as well as Dr. Valérie Payré for insightful comments. This is CRPG contribution number 2837. This is ClercVolc contribution number 578.

References

Adams, J. B., & Goullaud, L. H. (1978). Plagioclase feldspars: Visible and near infrared diffuse reflectance spectra as applied to remote sensing. *Proceedings of the Lunar and Planetary Science Conference*, *9*, 2901–2909.

Barthez, M., Flahaut, J., Guitreau, M., Pik, R., & Ito, G. (2022). Reflectance spectroscopy and optical microscopy laboratory analyses of terrestrial feldspathic rocks as analogs to Mars. *EPSC*, *16*, EPSC2022–467.

Beyer, R. A., Alexandrov, O., & McMichael, S. (2018). The Ames stereo pipeline: NASA's open source software for deriving and processing terrain data. *Earth and Space Science*, *5*(9), 537–548. https://doi.org/10.1029/2018ea000409

Bibring, J. P., Langevin, Y., Mustard, J. F., Poulet, F., Arvidson, R., Gendrin, A., et al. (2006). Global mineralogical and aqueous Mars history derived from OMEGA/Mars Express data. *Science*, *312*(5772), 400–404. https://doi.org/10.1126/science.1122659

Bouvier, L. C., Costa, M. M., Connelly, J. N., Jensen, N. K., Wielandt, D., Storey, M., et al. (2018). Evidence for extremely rapid magma ocean crystallization and crust formation on Mars. *Nature*, *558*(7711), 586–589. https://doi.org/10.1038/s41586-018-0222-z

Brustel, C., Flahaut, J., Hauber, E., Fueten, F., Quantin, C., Stesky, R., & Davies, G. R. (2017). Valles Marineris tectonic and volcanic history inferred from dikes in eastern Coprates Chasma. *Journal of Geophysical Research: Planets*, *122*(6), 1353–1371. https://doi.org/10.1002/2016je005231

Carter, J., & Poulet, F. (2013). Ancient plutonic processes on Mars inferred from the detection of possible anorthositic terrains. *Nature Geoscience*, *6*(12), 1008–1012. https://doi.org/10.1038/ngeo1995

Cheek, L. C., & Pieters, C. M. (2014). Reflectance spectroscopy of plagioclase-dominated mineral mixtures: Implications for characterizing lunar anorthosites remotely. *American Mineralogist*, *99*(10), 1871–1892. https://doi.org/10.2138/am-2014-4785

Crown, D. A., & Pieters, C. M. (1987). Spectral properties of plagioclase and pyroxene mixtures and the interpretation of lunar soil spectra. *Icarus*, *72*(3), 492–506. https://doi.org/10.1016/0019-1035(87)90047-9

Edwards, C. S., Nowicki, K. J., Christensen, P. R., Hill, J., Gorelick, N., & Murray, K. (2011). Mosaicking of global planetary image datasets: 1. Techniques and data processing for thermal emission imaging system (THEMIS) multi-spectral data. *Journal of Geophysical Research*, *116*(E10), E10008. https://doi.org/10.1029/2010je003755

Elkins-Tanton, L. T., Hess, P. C., & Parmentier, E. M. (2005). Possible formation of ancient crust on Mars through Magma Ocean processes. *Journal of Geophysical Research*, *110*(E12), E12S01. https://doi.org/10.1029/2005je002480

Farrand, W. H., Rice, J. W., Jr., Chuang, F. C., & Rogers, A. D. (2021). Spectral and geological analyses of domes in western Arcadia Planitia, Mars: Evidence for intrusive alkali-rich volcanism and ice-associated surface features. *Icarus*, *357*, 114111. https://doi.org/10.1016/j.icarus.2020.114111

Flahaut, J., Mustard, J. F., Quantin, C., Clenet, H., Allemand, P., & Thomas, P. (2011). Dikes of distinct composition intruded into Noachian-aged crust exposed in the walls of Valles Marineris. *Geophysical Research Letters*, *38*(15). https://doi.org/10.1029/2011gl048109

Flahaut, J., Quantin, C., Clenet, H., Allemand, P., Mustard, J. F., & Thomas, P. (2012). Pristine Noachian crust and key geologic transitions in the lower walls of Valles Marineris: Insights into early igneous processes on Mars. *Icarus*, *221*(1), 420–435. https://doi.org/10.1016/j.icarus.2011.12.027

Fraeman, A. A., Rapin, W., Bapst, J., Matthies, L. H., Ehlmann, B. L., Golombek, M. P., et al. (2022). Science enabled by aerial explorers: Addressing outstand questions in the Martian geological record. In *Low-cost science mission concepts workshop*. abstract #5045.

Fueten, F., Stesky, R., MacKinnon, P., Hauber, E., Zegers, T., Gwinner, K., et al. (2008). Stratigraphy and structure of interior layered deposits in west Candor Chasma, Mars, from high resolution stereo camera (HRSC) stereo imagery and derived elevations. *Journal of Geophysical Research*, *113*(E10), E10008. https://doi.org/10.1029/2007je003053

Fueten, F., Stesky, R. M., & MacKinnon, P. (2005). Structural attitudes of large scale layering in Valles Marineris, Mars, calculated from Mars orbiter laser altimeter data and Mars orbiter camera imagery. *Icarus*, *175*(1), 68–77. https://doi.org/10.1016/j.icarus.2004.11.010

Ito, G., Flahaut, J., Gonzalez-Maurel, O., Godoy, B., Payet, V., & Barthez, M. (2022). Remote sensing Survey of altiplano-Puna volcanic complex rocks and minerals for planetary analog use. *Remote Sensing*, *14*(9), 2081. https://doi.org/10.3390/rs14092081

Kokaly, R. F., Clark, R. N., Swayze, G. A., Livo, K. E., Hoefen, T. M., Pearson, N. C., et al. (2017). USGS spectral library version 7: U.S. *Geological Survey Data Series*, *1035*, 61. https://doi.org/10.3133/ds1035

McGuire, P. C., Bishop, J. L., Brown, A. J., Fraeman, A. A., Marzo, G. A., Frank Morgan, M., et al. (2009). An improvement to the volcano-scan algorithm for atmospheric correction of CRISM and OMEGA spectral data. *Planetary and Space Science*, *57*(7), 809–815. https://doi.org/10.1016/j.pss.2009.03.007

McSween, H. Y., Grove, T. L., & Wyatt, M. B. (2003). Constraints on the composition and petrogenesis of the Martian crust. *Journal of Geophysical Research*, *108*(E12). https://doi.org/10.1029/2003je002175

McSween, H. Y., Jr., Taylor, G. J., & Wyatt, M. B. (2009). Elemental composition of the Martian crust. *Science*, *324*(5928), 736–739. https://doi.org/10.1126/science.1165871

Milliken, R. E., Hiroi, T., & Patterson, W. (2016). The NASA reflectance experiment laboratory (RELAB) facility: Past, present, and future. In *47th lunar and planetary science conference*. abstract #2058.

Murchie, S., Arvidson, R., Bedini, P., Beisser, K., Bibring, J. P., Bishop, J., et al. (2007). Compact reconnaissance imaging spectrometer for Mars (CRISM) on Mars reconnaissance orbiter (MRO). *Journal of Geophysical Research*, *112*, E5.

Nash, D. B., & Conel, J. E. (1974). Spectral reflectance systematics for mixtures of powdered hypersthene, labradorite, and ilmenite. *Journal of Geophysical Research*, *79*(11), 1615–1621. https://doi.org/10.1029/jb079i011p01615

Pangaea Scientific. (2006). Orion: Orientation Hunter [Computer software]. Supported by Canada centre for remote sensing, natural resources Canada. https://www.cloudynights.com/topic/752506-orion-the-hunter/

Payet, V., Flahaut, J., Ito, G., Barthez, M., & Breton, S. (2020). Automated denoising for mineral identification on hyperspectral data. In *The eleventh Moscow solar system symposium (11M-S3) (virtual)*. abstract 11MS3- MS-PS-06.

Phillips, M. S., Viviano, C. E., Moersch, J. E., Rogers, A. D., McSween, H. Y., & Seelos, F. P. (2022). Extensive and ancient feldspathic crust detected across north Hellas rim, Mars: Possible implications for primary crust formation. *Geology*, *50*(10), 1182–1186. https://doi.org/10.1130/g50341.1

Pik, R., Deniel, C., Coulon, C., Yirgu, G., Hofmann, C., & Ayalew, D. (1998). The Northwestern Ethiopian Plateau flood basalts: Classification and spatial distribution of magma types. *JVGR*, *81*(1–2), 91–111. https://doi.org/10.1016/s0377-0273(97)00073-5

Quantin, C., Flahaut, J., Clenet, H., Allemand, P., & Thomas, P. (2012). Composition and structures of the subsurface in the vicinity of Valles Marineris as revealed by central uplifts of impact craters. *Icarus*, *221*(1), 436–452. https://doi.org/10.1016/j.icarus.2012.07.031

Quantin-Nataf, C., Lozac'h, L., Thollot, P., Loizeau, D., Bultel, B., Fernando, J., et al. (2018). MarsSI: Martian surface data processing information system. *Planetary and Space Science*, *150*, 157–170. https://doi.org/10.1016/j.pss.2017.09.014

Rogers, A. D., & Farrand, W. H. (2022). Spectral evidence for alkaline rocks and compositional diversity among feldspathic light-toned terrains on Mars. *Icarus*, *376*, 114883. https://doi.org/10.1016/j.icarus.2022.114883

Rogers, A. D., & Nekvasil, H. (2015). Feldspathic rocks on Mars: Compositional constraints from infrared spectroscopy and possible formation mechanisms. *Geophysical Research Letters*, *42*(8), 2619–2626. https://doi.org/10.1002/2015gl063501

Sautter, V., Toplis, M. J., Beck, P., Mangold, N., Wiens, R., Pinet, P., et al. (2016). Magmatic complexity on early Mars as seen through a combination of orbital, in-situ and meteorite data. *Lithos*, *254–255*, 25436–25452. https://doi.org/10.1016/j.lithos.2016.02.023

Sautter, V., Toplis, M. J., Wiens, R. C., Cousin, A., Fabre, C., Gasnault, O., et al. (2015). In situ evidence for continental crust on early Mars. *Nature Geoscience*, *8*(8), 605–609. https://doi.org/10.1038/ngeo2474

Smith, D. E., Zuber, M. T., Frey, H. V., Garvin, J. B., Head, J. W., Muhleman, D. O., et al. (2001). Mars Orbiter laser altimeter—Experiment summary after the first year of global mapping of Mars. *Journal of Geophysical Research*, *106*(E10), 23689–23722. https://doi.org/10.1029/2000je001364

Viviano-Beck, C. E., Seelos, F. P., Murchie, S. L., Kahn, E. G., Seelos, K. D., Taylor, H. W., et al. (2014). Revised CRISM spectral parameters and summary products based on the currently detected mineral diversity on Mars. *Journal of Geophysical Research: Planets*, *119*(6), 1403–1431. https://doi.org/10.1002/2014JE004627

Viviano-Beck, C. E., Murchie, S. L., Beck, A. W., & Dohm, J. M. (2017). Compositional and structural constraints on the geologic history of eastern Tharsis Rise, Mars. *Icarus*, *284*, 43–58. https://doi.org/10.1016/j.icarus.2016.09.005

Williams, J. P., Paige, D. A., & Manning, C. E. (2003). Layering in the wall rock of Valles Marineris: Intrusive and extrusive magmatism. *Geophysical Research Letters*, *30*(12), 1623. https://doi.org/10.1029/2003gl017662

Wray, J. J., Hansen, S. T., Dufek, J., Swayze, G. A., Murchie, S. L., Seelos, F. P., et al. (2013). Prolonged magmatic activity on Mars inferred from the detection of felsic rocks. *Nature Geoscience*, *6*(12), 1013–1017. https://doi.org/10.1038/ngeo1994